

High performance PZT capacitor using highly crystalline SRO bottom electrode for Mbit FeRAM devices

Hiroshi Itokawa, Katsuaki Natori, Soichi Yamazaki, Gerhard Beitel¹ and Koji Yamakawa

Semiconductor Company, Toshiba Corp., 8 Shinsugita-cho, Isogo-ku, Yokohama, 235-8522 Japan

¹ Infineon Technologies Japan, 8 Shinsugita-cho, Isogo-ku, Yokohama, 235-8522 Japan

Phone: +81-45-770-3675 Fax: +81-45-770-3577 E-mail: itokawa@amc.toshiba.co.jp

1. Introduction

Advantages of $\text{Pb}(\text{Zr,Ti})\text{O}_3$ (PZT) capacitors with SrRuO_3 (SRO) electrodes in comparison with Pt/PZT/Pt capacitors are higher endurance, lower coercive voltage, better polarization saturation property and more uniform small PZT grains^[1]. It is necessary to improve PZT film properties furthermore for achieving smaller capacitor cells and lower operation voltage in high-density FeRAM devices. The key to improvement of PZT film properties is crystallinity and morphology control of SRO bottom electrodes.

In this paper, we describe the improvement of SRO films and PZT capacitors in terms of structural and electrical properties.

2. Experimental

SRO films were deposited by DC sputtering on Pt/Ti/SiO₂/Si. PZT films were formed by RF sputtering followed by crystallization RTP at 650°C in oxygen flow. Pt/SRO top electrodes were DC sputter deposited with crystallization RTP at 650°C in oxygen. The crystallinity, microstructure, hysteresis property, fatigue and imprint characteristics were investigated using transmission electron microscopy (TEM), X-ray diffraction (XRD) and RT 6000S ferroelectric tester.

3. Results and discussion

One of the keys to SRO bottom electrodes is its crystallinity and morphology control. Figure 1(a) shows a cross-sectional TEM image of SRO deposited on Pt. Well-crystallized SRO film with smooth surface is shown in Fig. 1(a) and the inset of that. Fig. 1(b) presents a cross-sectional TEM image of PZT film formed on the SRO film. It is found that there is a well crystallized distinct SRO layer with a lattice matched interface between PZT and Pt. The PZT has columnar grains. Fig. 1(c) shows XRD diffraction pattern for 110nm PZT film formed on the SRO bottom electrode. $\langle 111 \rangle$ preferred oriented PZT film can be obtained. The PZT capacitor has large switching charge of 50.4 $\mu\text{C}/\text{cm}^2$ at 2.5V and square hysteresis shape (Fig. 1(d)). Figure 2 shows the properties of different SRO with poor crystallinity and PZT films. In this case, the SRO film consists of SrO and Ru, as shown in Fig. 2(a) and the inset of that. The PZT/SRO interface is ambiguous and PZT has granular grains, as shown in Fig. 2(b). Fig. 2(c) indicates XRD diffraction pattern for 110nm PZT film formed on the mixed crystalline SRO bottom electrode. The PZT film with the SRO is randomly oriented. The PZT capacitor has small switching charge of 28.7 $\mu\text{C}/\text{cm}^2$ at 2.5V and slanted hysteresis loop, as shown in Fig. 2(d). From these results, it is confirmed that the key to improve hysteresis property is to obtain well-crystallized uniform SRO films with

no decomposition and smooth surfaces.

Since the interface between PZT and electrodes dominates the reliability of PZT capacitors, we evaluated imprint and fatigue properties of PZT capacitors. Figure 3 exhibits the change in switching charge of 110nm PZT capacitor with well-crystallized SRO and that with mixed crystalline SRO after aging at 150°C as an imprint test. The PZT capacitor with mixed crystalline SRO extremely degrades, while the PZT capacitor with well-crystallized SRO shows only 15% decrease in switching charge after 100 hours at 150°C. Figure 4 indicates the fatigue property of the PZT capacitor with well-crystallized SRO. Fatigue free beyond 1E10 cycles property is achieved. We believe that lattice matched PZT/SRO interface with less defects by well-crystallized SRO forms less space charges at the interface resulting in good imprint property with no fatigue.

We tried PZT film thickness reduction for low voltage operation of the capacitors using the newly developed PZT/SRO structures. 85nm PZT capacitor shows a well-saturated hysteresis loop and good switching charge, as shown in figure 5. The switching charge is 32.4 $\mu\text{C}/\text{cm}^2$ with a leakage current of 1.8E-7A/cm² at 1.5V. This shows the possibility to apply the new process for future low voltage FeRAMs.

We also adapted the well-crystallized SRO film on Ir based bottom electrode. Since an Ir film has good diffusion barrier properties against oxygen, Ir based bottom electrode is essential for high-density FeRAM capacitors with COP (capacitor on plug) structure. However, there was a problem that PZT capacitor with SRO directly formed on Ir had large leakage current^[2]. Figure 6 shows the hysteresis loop of 110nm PZT film formed on well-crystallized SRO/Ir/Ti bottom electrode. The leakage current degradation is strongly suppressed and the PZT capacitor has large enough switching charge of 63.6 $\mu\text{C}/\text{cm}^2$ with a leakage current of 7.0E-5A/cm² at 2.5V and square hysteresis loop. It is expected that the well-crystallized SRO film can avoid the interface degradations such as counter diffusion and morphological degradation.

4. Conclusions

Well-crystallized uniform SRO with no phase separation is of considerable importance to improve the hysteresis property of PZT capacitor. The new process leads to excellent ferroelectric properties and reliable behaviors in terms of imprint and fatigue characteristics.

Acknowledgements

The authors would like to thank all members of the FeRAM Development Alliance between Toshiba and Infineon for fruitful discussion.

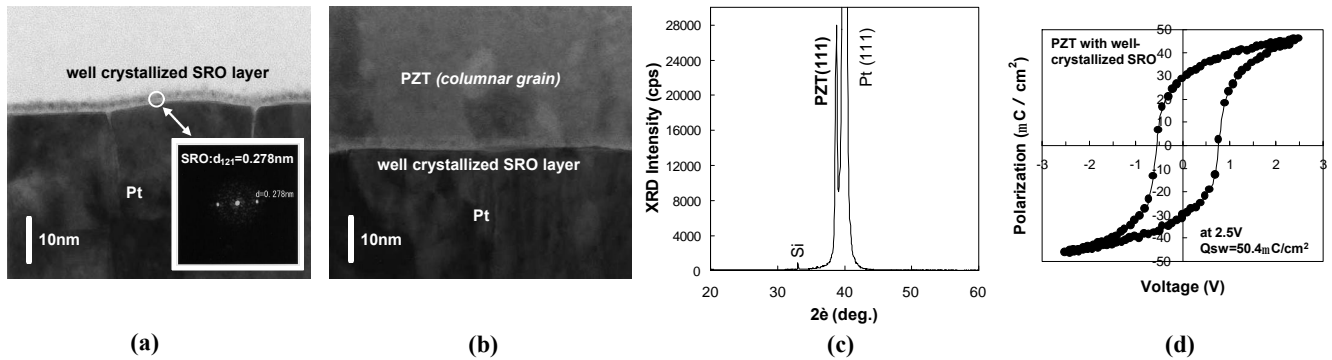


Figure 1 (a) Cross-sectional TEM image of well-crystallized SRO formed on Pt. (b) Cross-sectional TEM image, (c) XRD pattern and (d) hysteresis loop of 110nm PZT film formed on well-crystallized SRO/Pt/Ti bottom electrode.

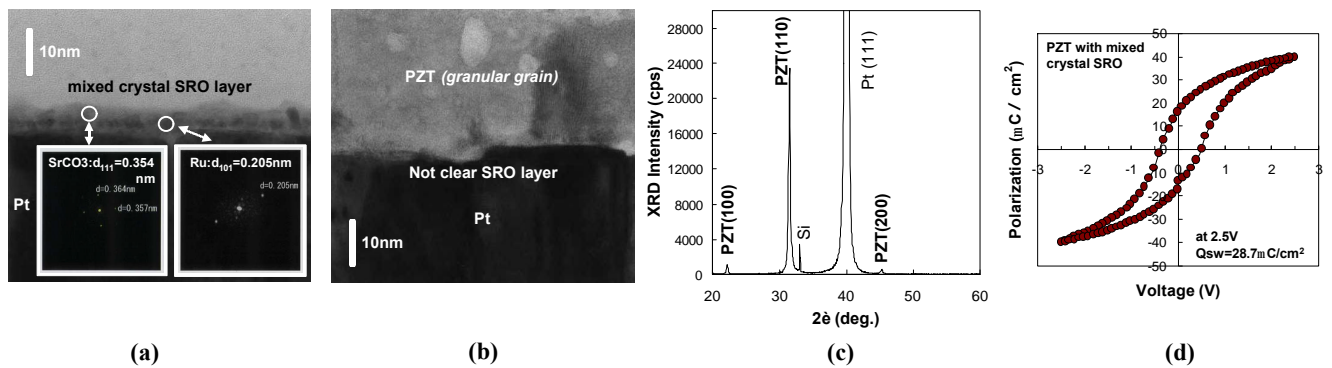


Figure 2 (a) Cross-sectional TEM image of mixed crystal SRO formed on Pt. (b) Cross-sectional TEM image, (c) XRD pattern and (d) hysteresis loop of 110nm PZT film formed on mixed crystal SRO/Pt/Ti bottom electrode.

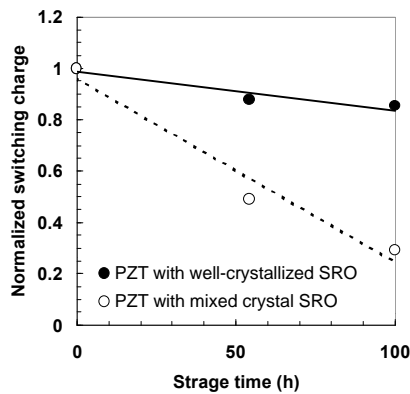


Figure 3 Imprint as a function of stress time at 150 .

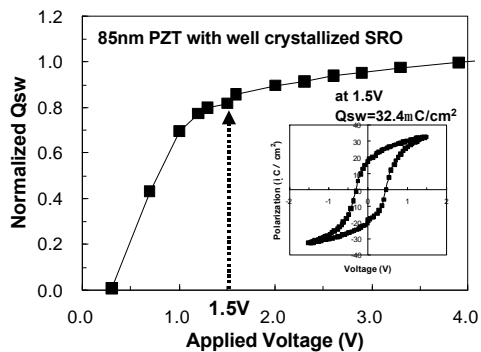


Figure 5 Saturation characteristic and hysteresis curve for 85nm PZT capacitor with well-crystallized SRO/Pt/Ti.

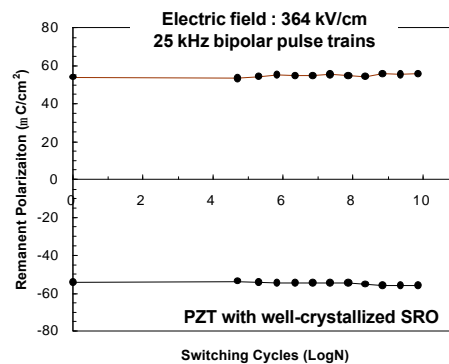


Figure 4 Fatigue performance of PZT capacitor with well-crystallized SRO/Pt/Ti bottom electrode.

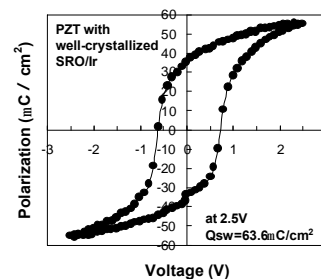


Figure 6 Hysteresis loop for 110nm PZT capacitor with well-crystallized Ir/Ti bottom electrode.

[Reference]

- [1]T. Morimoto, et al., Jpn. J. Appl. Phys.,**39** (2000) 2110-2113.
- [2]K. Yamakawa, et al., Integrated Ferroelectrics, **39**, (2001) 981.